https://doi.org/10.5194/egusphere-2024-4069
Preprint. Discussion started: 16 January 2025

Bridging the polarimetric structure and lightning activity of an isolated thunderstorm during the cloud life cycle

Chuanhong Zhao,[1,2]* Yijun Zhang,[1,3]* Huiyan Zhai,[2] Zhe Li,[1] Dong Zheng,[4] Xueyan Peng,[2] Wen Yao,[4] Sai Du,[5] Yuanmou Du,[6]

Affiliations

[1]Department of Atmospheric and Oceanic Sciences & Institute of Atmospheric Sciences, Fudan University, Shanghai, 200438, China.

[2]Plateau Atmosphere and Environment Key Laboratory of Sichuan Province, School of Atmospheric Sciences, Chengdu University of Information Technology, Chengdu, 610225, China.

[3]Shanghai Key Laboratory of Ocean-land-atmosphere Boundary Dynamics and Climate Change & Shanghai Frontiers Science Center of Atmosphere-Ocean Interaction, Fudan University, Shanghai, 200438, China.

[4]State Key Laboratory of Severe Weather, Chinese Academy of Meteorological Sciences & Laboratory of Lightning Physics and Protection Engineering, Chinese Academy of Meteorological Sciences, Beijing, 100081, China.

[5]Guangdong Meteorological Service, Guangzhou, 510080, China.

[6]Beijing Weather Modification Center, Beijing, 100089, China.

Corresponding authors: Dr. Yijun Zhang & Dr. Chuanhong Zhao are the co-corresponding authors.

E-mail: zhangyijun@fudan.edu.cn; zch@cuit.edu.cn

https://doi.org/10.5194/egusphere-2024-4069
Preprint. Discussion started: 16 January 2025

Abstract

Cloud microphysics and dynamics produce lightning flashes, which can be detected as polarimetric structures by radar. Many studies have indicated that differential reflectivity (Z_{DR}) and specific differential phase (K_{DP}) columns, which serve as proxies for updraft strength, are related to lightning activity; moreover, the quantities of ice and supercooled liquid water strongly influence the occurrence of lightning flashes via noninductive charging. However, few studies have focused on clarifying the sequence or interactions among these factors from the perspective of the cloud life cycle. Here, we establish the '3D mapping columns' method, which is based on the Cartesian grid datasets; this method is sensitive for identifying and quantifying the Z_{DR} columns in the early phase of cloud formation. Our study bridges the polarimetric structure and lightning activity within an isolated thunderstorm during the cloud life cycle. The results indicate that i) the parameter most relevant to total flashes/cloud-to-ground flashes is the content of supercooled rainwater/graupel. ii) The onset of the Z_{DR} column can be used to forecast lightning initiation in advance. iii) The signatures of the Z_{DR} and K_{DP} columns should be complementary and used to retrieve dynamic information instead of lightning activity. Notably, the variation in the Z_H intensity within Z_{DR} columns has high potential for predicting lightning activity during the cloud life cycle, which is valuable for exploration in the future. Our study improves the overall understanding of cloud microphysics and lightning activity, and suggestions for using these multiple polarimetric signatures to forecast severe weather are provided.

Short summary

Lightning activity is highly related to the signatures of polarimetric radar on the basis of cloud electrification physics. However, few studies have focused on bridging the polarimetric structure and lightning activity during the cloud life cycle. Here, we evaluated the sequence and interactions of polarimetric parameters for indicating lightning activity from the perspective of the cloud life cycle, and the cloud microphysics of the polarimetric structure was explored.

Keywords: thunderstorm; lightning activity; cloud microphysics; polarimetric radar

1.Introduction

Lightning is a traditional indication of severe weather (e.g., tornado, hail, microbursts, etc.). Trends in lightning activity are useful for determining the severity of a thunderstorm (e.g., Gatlin

https://doi.org/10.5194/egusphere-2024-4069
Preprint. Discussion started: 16 January 2025

and Goodman, 2010; Goodman, et al., 2005; Williams, et al., 1999; Zhang et al., 2009). Lightning activity is the electrical response to dynamic conditions (updraft or turbulence) and cloud microphysics during storm evolution, which is supported by both theoretical and field observational studies of dynamics, microphysics and lightning activity (lightning initiation or total lightning flash rate) (e.g., Baker, et al., 1999; Baker, et al., 1995; Carey and Rutledge, 2000; Mitzeva and Saunders, 1990; Souza and Bruning, 2021; Williams, et al., 1989; Zhang et al., 2004a; Zhao, et al., 2021). Notably, many studies have focused on the relationship between lightning activity and cloud updraft or microphysics (e.g., Carey and Rutledge, 1996, 2000; Deierling and Petersen, 2008; Lang and Rutledge, 2011; López and Aubagnac, 1997; Sharma, et al., 2024; Sharma, et al., 2021).

Polarimetric radar can provide observations to improve our understanding of the coupling between convective dynamics and storm microphysics (e.g., Sharma, et al., 2024). Lightning location technology can be used to monitor the occurrence of lightning flashes in real time (e.g., Rison, et al., 1999). In this way, radar and lightning observations can be used to link cloud updrafts and microphysics with lightning activity.

Carey and Rutledge (2000) utilized a C-band polarimetric radar to study the relationship between precipitation and lightning during tropical island convection events; their results indicated that lightning activity and the surface electric field are strongly correlated with the mixed-phase ice mass and rainfall properties during the mature phase of convection. Cloud-to-ground (CG) lightning was associated with the production and subsequent descent of graupel and frozen drops from the −10 to −20°C region; moreover, peaks in the CG lighting flash rate typically lagged behind peaks in the graupel mass aloft (Carey and Rutledge, 2000). This observational phenomenon reflects the noninductive charging between ice-phase hydrometeors, mainly graupel and ice crystals (e.g., Latham and Dye, 1989; Reynolds, et al., 1957; Saunders, 2008; Takahashi, 1978).

Before the formation of ice particles (e.g., graupel), the supercooled raindrops present in the mixed-phase zone throughout the developing and mature phases play crucial roles in storm kinematics, microphysics, and electrification. During freezing, supercooled raindrops likely provide (i) an instantaneous and abundant supply of millimetre-sized ice, (ii) a potential source of secondary ice particles, and (iii) an invigoration in the updraft due to the latent heat of freezing (Carey and Rutledge, 2000; Rosenfeld, et al., 2008; Zhao, et al., 2024; Zhao, et al., 2022). Moreover, millimetre-

https://doi.org/10.5194/egusphere-2024-4069
Preprint. Discussion started: 16 January 2025

sized ice and secondary ice particles contribute to cloud electrification (Bringi, et al., 1996; Sharma, et al., 2024). The intensity of convective updrafts through the modulation of microphysical factors, the collision efficiency of ice particles, and the electrification temperature influence the charge structure of storms (Liu, et al., 2024; Marshall, et al., 1995; Qie, et al., 2000; Yan et al., 1996a, b; Zhang, et al., 2004b), the flash size (Bruning and MacGorman, 2013; Zheng and Zhang, 2021), and the associated lightning flash rate (Deierling and Petersen, 2008; Deierling, et al., 2008; Fridlind, et al., 2019; Souza and Bruning, 2021; Zhao, et al., 2021).

Moreover, supercooled raindrops produce a differential reflectivity (Z_{DR}) column, one of the most notable polarimetric radar signatures of convective storms. High Z_{DR} values (e.g., >1 dB) above the 0°C isotherm height (freezing level) are associated with large supercooled raindrops and wet hail suspended in deep convective updrafts (e.g., Krause and Klaus, 2024; Kumjian, et al., 2014; Snyder, et al., 2015; Zhao, et al., 2020). Depending on the intensity of the updraft, the region of high Z_{DR} can extend several kilometres above the 0°C isotherm height. This narrow vertical extension of high Z_{DR} values above the environmental 0°C level associated with updrafts in strong convective storms is called the Z_{DR} column (Krause and Klaus, 2024; Kumjian, et al., 2014; Zhao, et al., 2020).

The Z_{DR} columns, due to the vertical size sorting of drops in warm-rain precipitation processes, encompass the signals of both microphysical features and updrafts; however, these signals are not present throughout the life cycle of strong convective storms, except in the early phase of cloud development. During the initial phase of a thunderstorm, the Z_{DR} column above the freezing level indicates the presence of a low concentration of large raindrops (>2 mm); in addition, the Z_{DR} column expands downwards from above due to the collision and coalescence of drops and the accretion of droplets, resulting in the formation of larger raindrops (>4–5 mm) (Kumjian, et al., 2014). During the mature phase of a thunderstorm, the Z_{DR} column above the freezing level may continue expanding upwards and outwards because stronger updrafts loft raindrops upwards into the mixed-phase layer, but smaller drops reach their nucleation temperature and begin to freeze while ascending to higher altitude. As these supercooled raindrops begin to freeze and mix with water-coated graupel and hail, the corresponding Z_{DR} values decrease, denoting top of the Z_{DR} column. As updrafts subsequently weaken and large ice particles (high-density graupel or hailstones) increase in abundance, the Z_{DR} column starts to collapse; however, lightning activity may exhibit

https://doi.org/10.5194/egusphere-2024-4069
Preprint. Discussion started: 16 January 2025

an inverse trend compared with that of the Z_{DR} column at this moment.

On the other hand, in the specific differential phase (K_{DP}) column, high values (>0.75°/km, the value reported by Loney et al. (2002)) above the freezing level occur and are strongly associated with a high concentration of water-coated ice (e.g., water-coated graupel and hail with a non-spherical shape) and raindrops (1–2 mm) that shed from hailstones growing in a wet regime (Bringi, et al., 1996; Hubbert, et al., 1998; Loney, et al., 2002). Thus, the formation of a K_{DP} column is tied to cold cloud microphysics, usually occurring later in the life cycle of a thunderstorm.

van Lier-Walqui et al. (2016) attempted to determine the constraints of cloud-resolving models on the basis of ground-based remote sensing observations, namely, polarimetric radar data. In their study, the K_{DP} column (specifically, the column volume) was strongly related to the updraft mass flux, lightning activity, and rainfall intensity in four deep convection events observed during the Midlatitude Continental Convective Clouds Experiment. Recently, Sharma et al. (2024) utilized polarimetric radar observations of three severe storms during the VORTEX-Southeast field campaign to quantify the correlation between the volumes of Z_{DR} and K_{DP} columns (representative of mixed-phase microphysics as well as updraft intensity and size) and total lightning flash rates. They indicated that the volume of the K_{DP} columns exhibited high co-variability with the total flash rate in three such cases (a tornadic supercell embedded in a stratiform precipitation system, a non-tornadic supercell, and a supercell embedded within a quasilinear convective system).

Sharma et al. (2024) conducted a study on the basis of hypotheses, namely, that the deeper and wider the Z_{DR} and K_{DP} columns were in cases with robust and wide updrafts (e.g., Homeyer and Kumjian, 2015; Snyder, et al., 2017), the more an increase in the volumes of the Z_{DR} and K_{DP} columns would correspond to an increase the mixed-phase ice mass flux, resulting in an increase in the total flash rate; therefore, the correlation coefficient (−0.47~0.37 for the Z_{DR} column; 0.54~0.74 for the K_{DP} column) between Z_{DR} or K_{DP} columns and lightning activity was not high. In addition, the effect of the time lag may decrease this correlation coefficient. As reported by Carey and Rutledge (2000), they obtained a very high one-lag (7 minutes) correlation coefficient (ρ = 0.9) between the graupel mass within the mixed-phase zone and the CG lightning flash rate, suggesting that the directly related microphysics with noninductive charging have a greater correlation coefficient with lightning activity.

https://doi.org/10.5194/egusphere-2024-4069
Preprint. Discussion started: 16 January 2025

In summary, four parameters derived from polarimetric radar can provide forecasting information about lightning activity on the basis of noninductive charging: i) the precipitation-sized (e.g., graupel) ice mass within the mixed-phase zone; ii) the content of supercooled raindrops; and iii) the quantified Z_{DR} and K_{DP} columns (e.g., the column volume or height). Our goal in this study is to link these four parameters for forecasting lightning activity within isolated thunderstorm cells during the cloud life cycle over South China, determine of whether the best proxy among these four parameters is used to forecast lightning activity, and determine how the cloud microphysics related to these four parameters should be assessed. Notably, the close relationship between these four parameters and lightning activity has been noted in many studies (e.g., Carey and Rutledge, 2000; Hayashi et al., 2021; Sharma et al., 2024; Sharma, et al., 2021; Snyder, et al., 2015; van Lier-Walqui, et al., 2016; Woodard et al., 2012); thus, we believe that this study is sufficient for connecting these four parameters and lightning activity via an isolated storm cell during the cloud life cycle.

This paper is organized as follows. In Section 2, an overview of the radar and lightning data is given, and the analysis methods and the approach for quantifying the Z_{DR}/K_{DP} columns are described. Section 3 presents the results of Z_{DR}/K_{DP} column quantification and the microphysical characteristics of the Z_{DR} column; additionally, the variation in the ice/water content within the mixed-phase zone with cloud development is illustrated, and the relationship between lightning activity and these polarimetric characteristics is presented. Finally, we summarize the results in Section 4.

2.Data and methodology

2.1. Radar and lightning observations

On 20 June 2016, one isolated thunderstorm cell was observed via an S-band dual-polarization radar deployed in Guangzhou city (GZ radar) (Figure 1). The composite reflectivity data revealed that this thunderstorm (the boundary was determined via manual inspection; the black lines in Figure 1) was nearly stationary and that the cloud life cycle lasted approximately two hours. Lightning activity occurred when values of composite reflectivity >35 dBZ were present; this phenomenon seemingly supported the results of Hayashi et al. (2021), highlighting the importance of graupel in cloud electrification.

The beam width of the GZ radar is ≤1°, and the azimuth and range resolutions are 1° and 250 m, respectively. A full radar volume scan lasted 6 minutes at nine elevation angles. The GZ radar

https://doi.org/10.5194/egusphere-2024-4069
Preprint. Discussion started: 16 January 2025

data were processed via the Python ARM Radar Toolkit (Py-ART), including quality control (Helmus and Collis, 2016; Li, et al., 2023; Li, et al., 2024). The Z_{DR} offset of the raw data was corrected via drizzle, and the calibration accuracy was expected to be 0.1–0.2 dB (Bringi and Chandrasekar, 2001). The radar data were gridded via Py-ART gridding routines on a Cartesian grid with a 0.25-km horizontal resolution and a 500-m vertical resolution ("Barnes2" method).

https://doi.org/10.5194/egusphere-2024-4069
Preprint. Discussion started: 16 January 2025

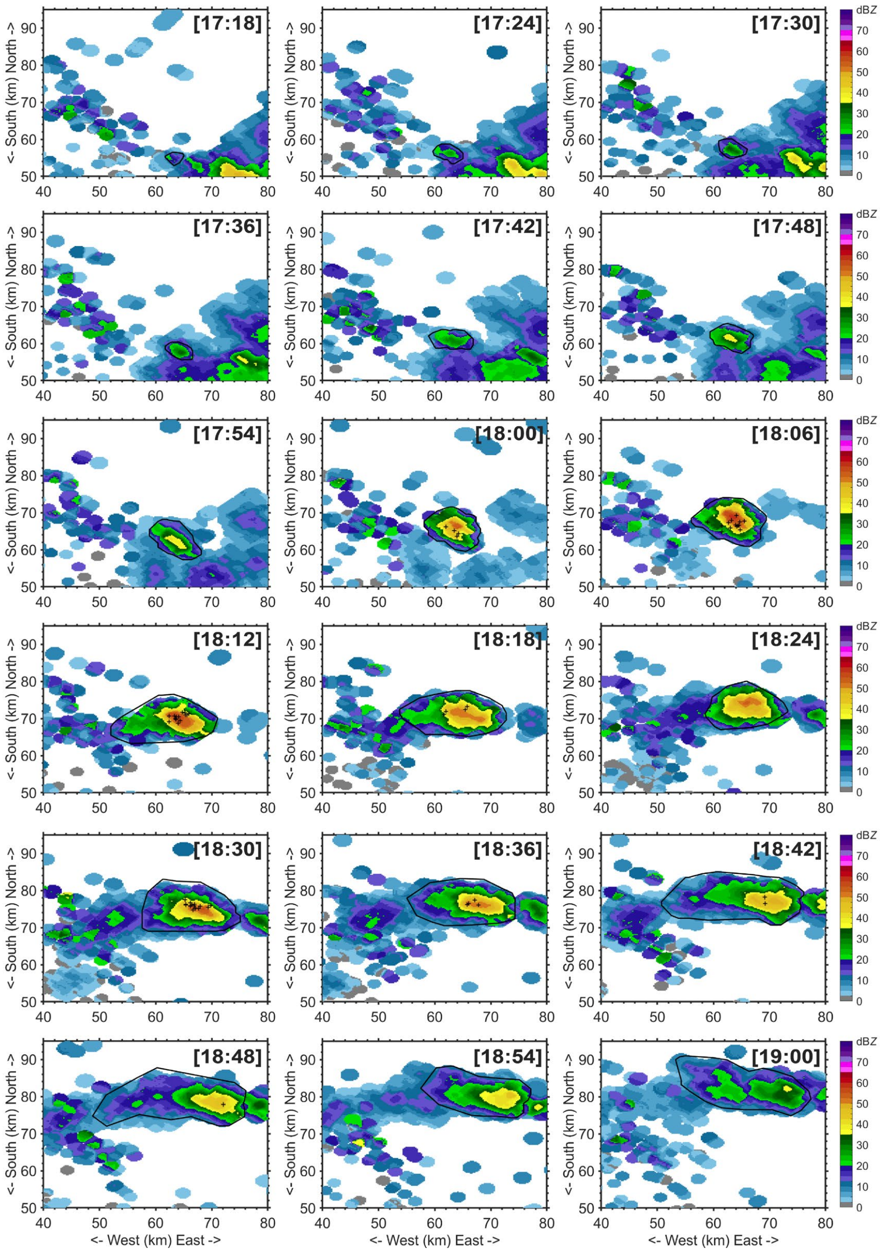

Figure 1. The composite reflectivity of the isolated thunderstorm cell on 20 June 2016, which initiated at 17:18 and ended at 19:00 (China Standard Time, CST). The black lines indicate the boundary of this thunderstorm. The black crosses indicate the lightning flashes, and the location of once lightning flash is represented by the location of the first discharge pulse event.

https://doi.org/10.5194/egusphere-2024-4069
Preprint. Discussion started: 16 January 2025

The lightning flashes within this thundercloud were detected via a low-frequency E-field detection array (LFEDA), which is a 3-D mapping detection system for intracloud and CG lightning, with 10 sensors. Previous studies (Fan, et al., 2018; Shi, et al., 2017) utilized information from triggered lightning flashes to evaluate LFEDA detection results; the results show the detection efficiency of the LFEDA can reach 100%, and the mean location error is 102 m. Discharge pulse events were grouped into a lightning flash via the same method as described by Liu et al. (2020). If any source within one lightning flash is below the 2-km height, this lightning flash was regarded as one cloud-to-ground flash, as suggested by Zhao et al. (2021).

The lightning flashes were assigned to the isolated thunderstorm on the basis of the boundary of the thunderstorm, as well as a constraint every 6 minutes (according to the duration of a full radar volume scan). The life cycle of this isolated thunderstorm initiated from the first radar echo (i.e., the presence of a maximum $Z_H \geq 5$ dBZ in a full radar volume scan within this cloud was first detected by the GZ radar, as suggested by Zhao et al. (2021, 2022, 2024)) and ended when the maximum Z_H started to decrease and Z_H reached ≤ 40 dBZ. The distributions of these detection systems, including radar and lightning location system, were illustrated by in Zhao et al. (2024).

2.2. Cloud microphysical parameter retrieval methods

To estimate the precipitation-sized ice mass (e.g., graupel, hail, and frozen drops) and the content of supercooled raindrops within the mixed-phase zone, an approach on the basis of difference reflectivity (Z_{DP}, dB) is applied (Carey and Rutledge, 2000). Pruppacher and Klett (1997) assumed that precipitation-sized ice particles were more spherically symmetrical or tumble. The low dielectric constant and significant canting behaviour of ice particles likely result in a near-zero Z_{DR} (e.g., Seliga and Bringi, 1976). Therefore, the horizontal reflectivity and vertical reflectivity are equal for ice particles, as "effective spheres", and Z_{DP} is solely influenced by raindrops.

If the relationship between horizontal reflectivity and Z_{DP} (raindrops) is known, the horizontal reflectivity of raindrops can be derived, and the residual difference in the observed horizontal reflectivity can be regarded as being associated with ice particles. The standard error for the relationship between horizontal reflectivity and Z_{DP} is consistently approximately 1 dB (Carey and Rutledge, 2000). The estimated ice mass from the horizontal reflectivity of ice particles is proportional to the actual ice mass and depends on the variability in the intercept parameter of an

https://doi.org/10.5194/egusphere-2024-4069
Preprint. Discussion started: 16 January 2025

assumed inverse exponential distribution for ice and the ice density; thus, the trends of the estimated ice mass are deemed sufficient to investigate lightning activity.

The estimated ice masses are assigned to graupel masses on the basis of scattering properties, namely, where the Z_H values exceed 35 dBZ (Carey and Rutledge, 2000; Kumjian, 2013a, b; Zhao, et al., 2021). The rain water content above the freezing level (0°C isotherm height; sounding data from the Qingyuan meteorological observatory are used to obtain the environmental temperature) is defined as the supercooled raindrop mass.

Z_{DR} columns are associated with low concentration of large raindrops (>2 mm); thus, the median volume diameter D_0 of raindrops is retrieved via the method described by Hu and Ryzhkov (2022) to provide supporting evidence for identifying Z_{DR} columns. The fractional standard deviation of the D_0 estimation is approximately 10% (Hu and Ryzhkov, 2022).

2.3. Previous automatically identification and quantification methods for Z_{DR}/K_{DP} columns

Currently, a few methods are available to automatically identify and quantify Z_{DR}/K_{DP} columns (e.g., Woodard et al., 2012; Krause and Klaus, 2024; Sharma, et al., 2024; Snyder, et al., 2015; van Lier-Walqui, et al., 2016). These methods are constructed on the basis of the morphology of the Z_{DR}/K_{DP} columns and/or the high values (e.g., Z_{DR} >1 dB; K_{DP}>1°/km) above the freezing level.

In the stage of cloud formation, high Z_{DR} values above the freezing level are simply used to identify Z_{DR} columns; however, these high values are not always associated with the Z_{DR} columns. Notably, three-body scatter signatures (Zrnić, 1987), depolarization streaks associated with the canting behaviour of ice in regions of strong electrification (Kumjian, 2013c), and oblate ice particles can lead to enhanced positive Z_{DR} values (Kumjian, 2013a). Thus, additional requirements were imposed to avoid identification errors, e.g., the reflectivity threshold value (Z_H ≥40 dBZ) (Woodard et al., 2012) and the height should be below the homogeneous freezing level, and the maximum height of the Z_{DR} column should be associated with the height at which Z_{DR} displays a negative vertical gradient (van Lier-Walqui, et al., 2016).

Recently, Krause and Klaus (2024) utilized the hotspot technique to identify the base of the Z_{DR} column on the basis of constant altitude plan projection indicators (CAPPIs). Although their results indicated an improvement in the plan region identified on the basis of the Z_{DR} column approach over the results of two different existing algorithms (Thunderstorm Risk Estimation from

https://doi.org/10.5194/egusphere-2024-4069
Preprint. Discussion started: 16 January 2025

Nowcasting Development via Size Sorting algorithm and the algorithm introduced by Snyder et al. (2015)), the depth and volume information for Z_{DR} columns was lost, which was not beneficial for forecasting lightning activity. In addition, the reflectivity threshold value (Z_H >25 dBZ) was required in this algorithm. Sharma et al. (2024) used an algorithm in the "scikit-image" Python package to identify Z_{DR}/K_{DP} columns from Cartesian grid data via threshold values ($Z_{DR} \geq 1$ dB; $K_{DP} \geq 1$°/km); they restricted the Z_H values to exceed 20 dBZ, and any instances of obvious data contamination or unrealistic values during the gridding process were manually removed prior to analysis. They focused on three supercells during lightning activity, and violent convection in such case will ignore the formation of Z_{DR}/K_{DP} columns at weak echo intensities, i.e., in the initiation stage of convective clouds.

2.4. Automatic 3D mapping of Z_{DR}/K_{DP} columns during the life cycle of an isolated cell storm

Our objective in this study is to explore the performance of microphysics retrieved via radar for forecasting lightning activity within isolated thunderstorm cells during the cloud life cycle. As depicted in Figure 1, our radar observations indicate that before the initiation of lightning, the echo intensity is weak during the early stage of a cloud. Moreover, we seek to determine whether Z_{DR} columns form in the early stages of cloud formation. In addition, K_{DP} columns are representative of small drops with high concentration shed from large ice particles (e.g., hailstones) growing in a wet regime (Hubbert, et al., 1998; Loney, et al., 2002); thus, are K_{DP} columns absent in the initial stage of convective cloud formation and even in early stages of lightning activity?

Figure 2 shows the first appearance of the Z_{DR} column at 17:24 (China Standard Time, CST), which is ~36 minutes earlier than the first lightning occurrence and only lags behind the first radar echo by 6 minutes. The high values of Z_{DR} extend to the mixed-phase region from the cloud bottom, and the height of the Z_{DR} column is approximately 1 km (Figure 2c). The corresponding Z_H values are smaller than 30 dBZ, but with the values of the co-polar correlation coefficient (CC) are relatively high (Figure 2a, d). These characteristics indicate the presence of large raindrops with low concentrations; the low K_{DP} values and large size of raindrops (exceeding 2 mm) support that (Figure 2e, f), we illustrate the microphysical structure corresponding to high Z_{DR} values in Figure 2b. The threshold value for identifying the Z_{DR} column in this study is 1.5 dB, considering that the size of raindrops should exceed 2 mm within the Z_{DR} column during the initial phase of a storm

https://doi.org/10.5194/egusphere-2024-4069
Preprint. Discussion started: 16 January 2025

(e.g., Kumjian, et al., 2014). In addition, the K_{DP} column is absent in the initial phase of this storm, not appearing until 18:30 CST.

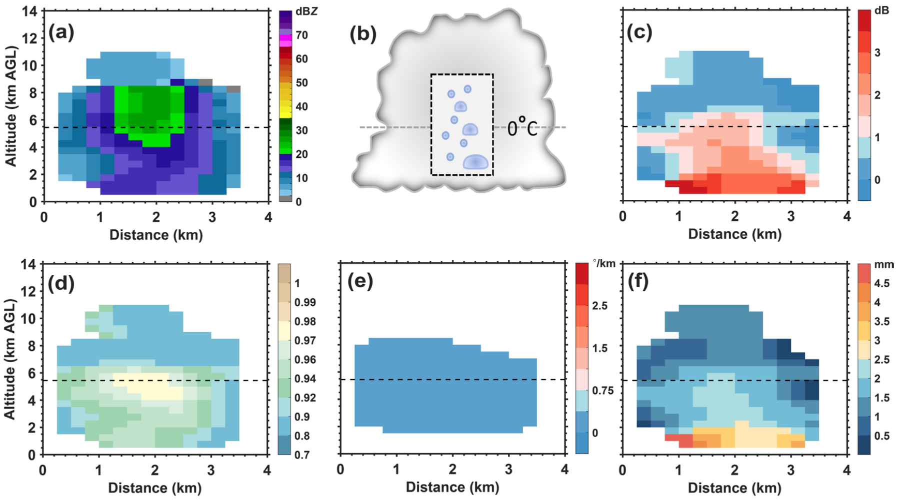

Figure 2. Cross section from the Cartesian grid of the studied isolated thunderstorm at 17:24 CST. (a) Z_H. (b) Conceptual model of the microphysical structure within high Z_{DR} values. (c) Z_{DR}, (d) CC, (e) K_{DP}. (f) Median volume diameter D_0 of raindrops. The black dashed line indicates the 0°C isotherm height.

In this study, we establish a method that only depends on the Z_{DR} parameter for identifying and easily quantifying the Z_{DR} column (e.g., height and volume) during the whole life cycle of a storm, specifically, including the initial phase of a convective cloud; the morphology of the Z_{DR} column resulted by size sorting and the high Z_{DR} values (≥1.5 dB) in Cartesian grid data are combined as the basis of this method. A flow chart of this method is depicted in Figure 3.

First, we establish logic matrices with the same specifications as the Z_{DR} matrices and identify the layer that corresponds to the 0°C isotherm height (with sounding data used to determine the environmental temperature). Second, from the 1-km height below the freezing level to the mixed-phase region, if Z_{DR} ≥1.5 dB, the corresponding logic values in the logic matrix are equal to 1. Notably, we utilize the lower portion of the logic matrix to upwards restrict the possible errors associated with including locations outside the successive column of high Z_{DR} values (≥1.5 dB). This restriction condition is based on the column morphology (columnar shape), which results from drop size sorting. Specifically, the region of the Z_{DR} column contracts upwards from the 0°C isotherm height below the mixed-phase region (e.g., as shown in Amiot et al. (2019), Hubbert et al.

https://doi.org/10.5194/egusphere-2024-4069
Preprint. Discussion started: 16 January 2025

(2018), Kumjian et al. (2014), Snyder et al. (2015) and Tuttle et al. (1989)). In the Cartesian grid data, this phenomenon is particularly obvious (Figure 2c).

Third, the size distribution of raindrops within the Z_{DR} column is determined by size sorting; thus, we utilize the negative vertical gradient of Z_{DR} on the basis of every grid between two adjacent layers from the 0°C isotherm height to the uppermost limit height to further ensure that the grids are associated with the Z_{DR} column. Finally, a 3D mapping of the Z_{DR} column is constructed. We can use the grid information to compute the height and volume of the Z_{DR} column. Although the formation mechanism of the K_{DP} column is different from that of the Z_{DR} column, the morphology of the K_{DP} column is highly consistent with that of the Z_{DR} column; thus, this method can be applied to map the K_{DP} column with a 3D grid based on the threshold value for identifying the K_{DP} column (e.g., ≥1°/km).

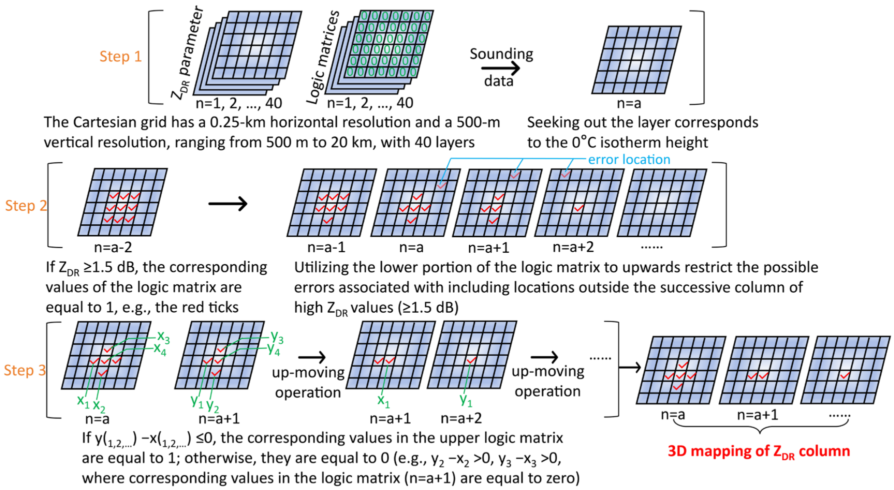

Figure 3. Flow chart of 3D mapping of a Z_{DR} column.

3.Results

3.1. Assessment of Z_{DR}/K_{DP} columns identified via the "3D mapping columns" method

Snapshots of the identified Z_{DR} columns via the "3D mapping columns" method at four moments (the K_{DP} column only existed at one moment during the life cycle of this thunderstorm) are shown in Figure 4. The identified regions of the Z_{DR}/K_{DP} columns are represented by white dots. We verify that the "3D mapping columns" method performs well in identifying the Z_{DR}/K_{DP} columns via manual inspection.

https://doi.org/10.5194/egusphere-2024-4069
Preprint. Discussion started: 16 January 2025

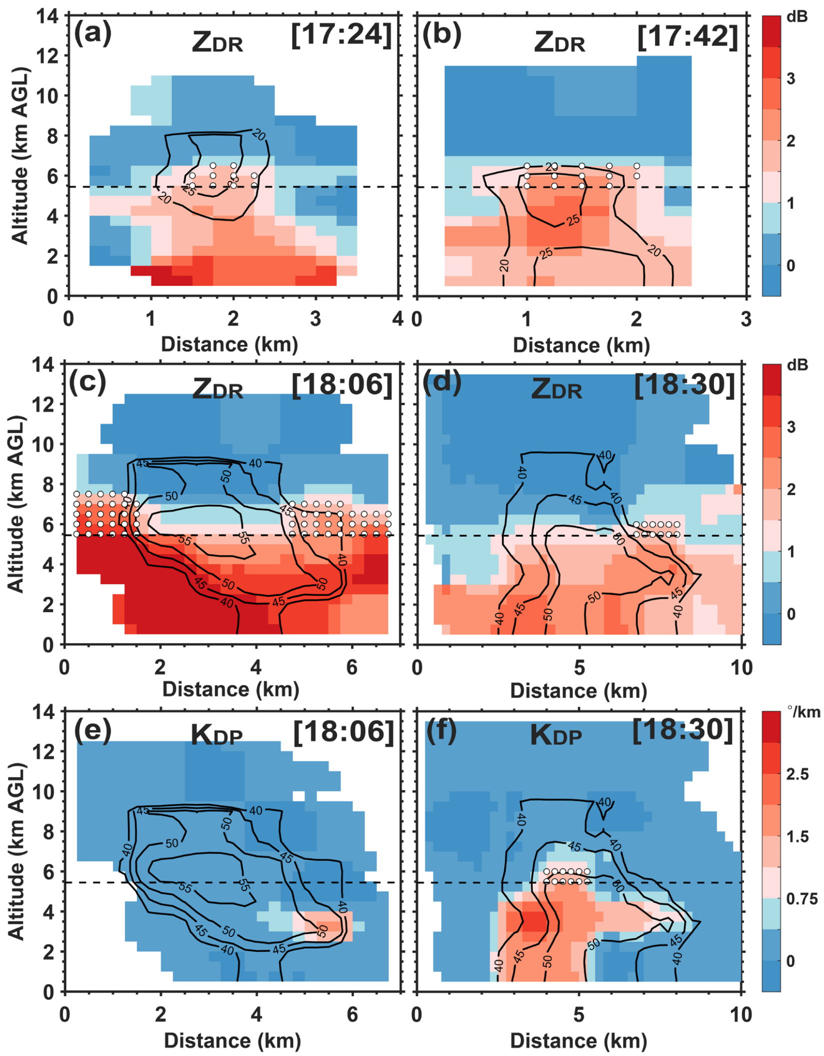

Figure 4. Cross sections from the Cartesian grid of the studied isolated thunderstorm at (a) 17:24 CST, Z_{DR}; (b) 17:42 CST, Z_{DR}; (c) 18:06 CST, Z_{DR}; (d) 18:30 CST, Z_{DR}; (e) 18:06 CST, K_{DP}; and (f) 18:30 CST, K_{DP}. The black dashed line indicates the 0°C isotherm height. The white dots indicate the areas of the identified Z_{DR}/K_{DP} columns. The black contours with values indicate the reflectivity structure.

The first Z_{DR} column in this isolated thunderstorm occurred at 17:24 CST (Figure 4a). The second Z_{DR} column subsequently occurred at 17:42 CST after 18 minutes (Figure 4b). At 18:06 CST, the lightning activity reached the first peak (Figure 5; to compare the radar and lightning data, the lightning flash frequency was counted every 6 minutes), and the Z_{DR} column was the highest and

https://doi.org/10.5194/egusphere-2024-4069
Preprint. Discussion started: 16 January 2025

largest (in volume) at this time. However, the overlap region between the Z_{DR} column and reflectivity core at 17:24 and 17:42 CST disappeared at 18:06 CST (Figure 4c); i.e., the Z_{DR} column within the reflectivity core began to collapse because of the falling of large-sized (represented by Z_H values exceeding 40 dBZ) ice particles.

Although large ice particles form and fall, the K_{DP} column is absent. However, a K_{DP} core with high values (≥1°/km) occurs near the location where large ice particles (approximately 50 dBZ) melt, and a shedding process occurs, resulting in a K_{DP} core. At 18:30 CST, the lightning activity reaches the second peak (Figure 5), but the Z_{DR} column almost disappears; interestingly, the K_{DP} column forms, with high values expanding downwards to the bottom of the cloud (Figure 4d, f). Thus, we suspect that K_{DP} column in this study may have formed on the basis of the raindrops (1–2 mm) shed from hailstones melting in the warm-phase region, which recirculated into the updrafts and were lifted to the mixed-phase region.

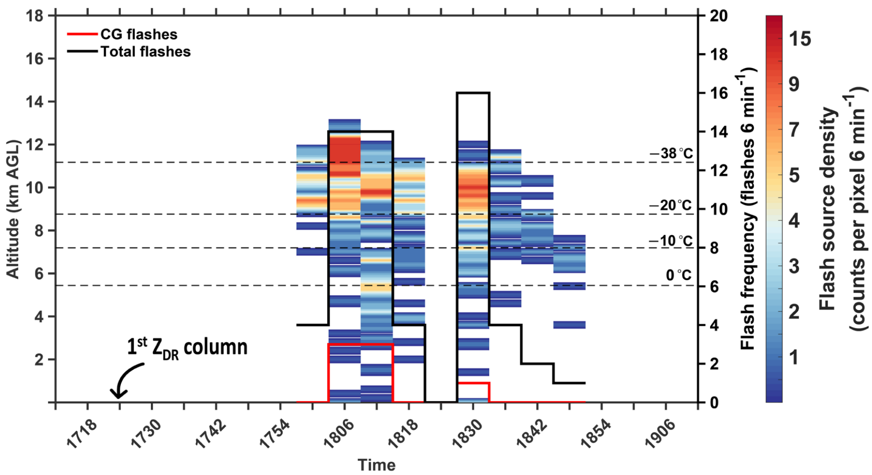

Figure 5. Time–height variation in flash source density (count per pixel, 6 min^{-1}). The black (red) stepped line indicates the total flashes (CG flashes) from the LFEDA. The dashed lines indicate the isotherm heights from 0 to −38°C.

3.2. The polarimetric and microphysical characteristics within the Z_{DR} columns

Figure 6 shows the normalized distributions of the polarimetric and microphysical characteristics within the series of Z_{DR} columns during the life cycle of the studied thunderstorm. The Z_H values within the Z_{DR} columns range from approximately 10 to 55 dBZ; specifically, weak reflectivity is present in the initial phase of the thundercloud (Figure 6a). This suggests the use of

https://doi.org/10.5194/egusphere-2024-4069
Preprint. Discussion started: 16 January 2025

the Z_H threshold value (e.g., 25, 40, or 35–50 dBZ) to help select Z_{DR} columns results in the loss of information, especially for the initial phase of clouds. The increase in reflectivity intensity within the Z_{DR} columns can be used to predict lightning activity, and the peaks in both reflectivity intensity and lightning activity are consistent. A strong reflectivity intensity peak is associated with a high number of lightning flashes (Figure 6a).

The Z_{DR} values within the Z_{DR} columns range from approximately 1.5 to 4 dB, and the increasing trend of the Z_{DR} values is consistent with the first peak of lightning activity but has a low correlation with the second peak of lightning activity (Figure 6b). The pattern of D_0 within the Z_{DR} columns is similar to that of the Z_{DR} values, depending on the strong linear relationship between D_0 and Z_{DR} (Figure 6c). The liquid water content within the Z_{DR} columns ranges from approximately 0.1 to 4 gm^{-3}, and the peaks correspond to the two peaks of lightning activity (Figure 6d). However, the relationship between the liquid water content within the Z_{DR} columns and the lightning flash frequency is not as strong as that between the Z_H values within the Z_{DR} columns and the lightning flash frequency.

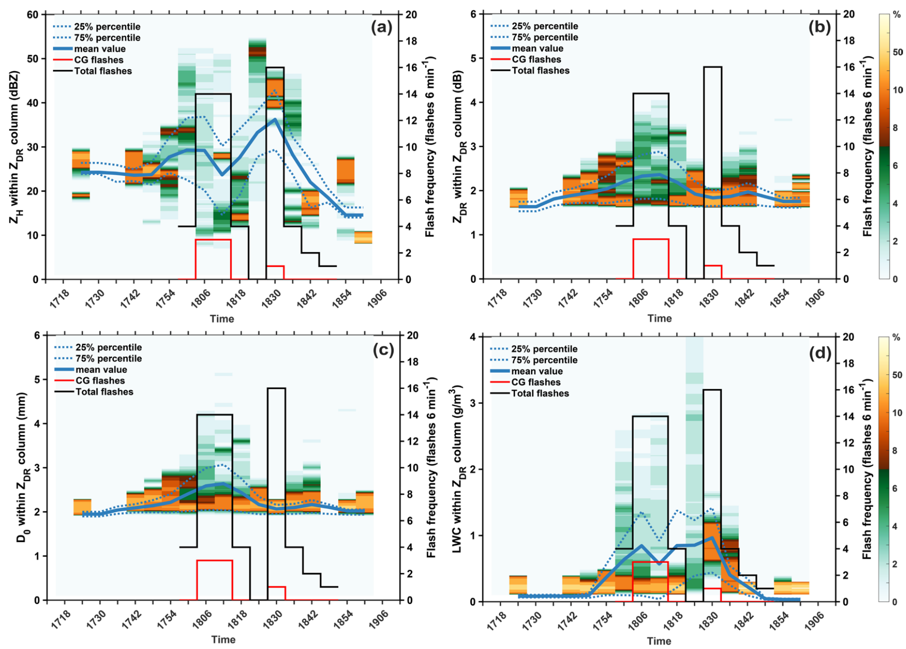

Figure 6. The normalized distributions of the polarimetric and microphysical characteristics within the series of Z_{DR} columns. (a) Z_H. (b) Z_{DR}. (c) Liquid water content (LWC). (d) Median volume diameter (D_0) of raindrops. The

https://doi.org/10.5194/egusphere-2024-4069
Preprint. Discussion started: 16 January 2025

blue solid line indicates the mean value. The blue dashed lines indicate the 25% and 75% percentiles. The black (red) stepped line indicates the total flashes (CG flashes) from LFEDA, and the lightning flash frequency is counted every 6 minutes.

In addition, the percentage of hydrometeors within the Z_{DR} columns is investigated on the basis of the retrieved contents of ice (including graupel) or raindrops, as described in Section 2b. The obvious phenomenon is that the percentage of graupel within the Z_{DR} columns suddenly peaks before the first peak of lightning activity, but the second peak of lightning activity is not related to the presence of graupel within the Z_{DR} columns; the hydrometeor type within the Z_{DR} column at 18:30 CST is raindrops (Figure 7). This indicate the collapse of the Z_{DR} column within the reflectivity core at 18:30 CST, which is consistent with the results shown in Figure 4d. On the other hand, the sudden increase in graupel within the Z_{DR} column at 18:00 CST may support the presence of a coalescence−freezing mechanism that led to graupel formation in the warm-based clouds. The hypothesis about coalescence−freezing mechanism was proposed in previous studies (e.g., Braham, 1986; Bringi, et al., 1997; Carey and Rutledge, 2000; Herzegh and Jameson, 1992).

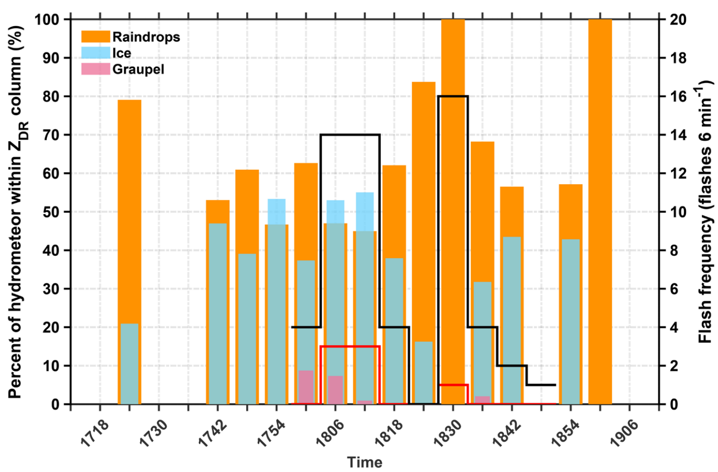

Figure 7. The percentages of hydrometeors within the series of Z_{DR} columns. The orange bars indicate the percentage of raindrops. The blue bars indicate the percentage of ice particles (including graupel). The pink bars indicate the percentage of graupel. The black (red) stepped line indicates the total flashes (CG flashes) from LFEDA, and the lightning flash frequency is counted every 6 minutes.

3.3. Relationship between lightning activity and quantified Z_{DR} columns

https://doi.org/10.5194/egusphere-2024-4069
Preprint. Discussion started: 16 January 2025

To determine the relationship between lightning activity and the quantified Z_{DR} columns, the height and volume of the Z_{DR} column are calculated via the "3D mapping column" method; the volume is based on the accumulation of all grids within the Z_{DR} column, and the volume of a single grid is 0.03125 km^3, with 0.25-km horizontal and 500-m vertical resolutions. The height of the Z_{DR} column is determined by counting the grid number (n) from the freezing level to the highest grid within the Z_{DR} column; if n is determined, the Z_{DR} column height is n×0.5 km.

Figure 8a displays the variations in the lightning flash frequency and Z_{DR} column height. The variation trend of the lightning activity before the second peak is highly consistent with the trend of the Z_{DR} column height. However, these trends seem to be in sync, which is not beneficial for forecasting lightning activity. The cross-correlation approach can be used to examine the correlation considering the time lag, which is important for verifying whether a parameter is appropriate for forecasting another parameter. Figure 8b shows the cross-correlation between lightning activity and the Z_{DR} column height. The highest correlation coefficient (~≤0.8) between lightning activity and the Z_{DR} column height is observed at a lag time of −6 minutes; thus, the variation in lightning activity occurs before that in the Z_{DR} column height (Figure 8b).

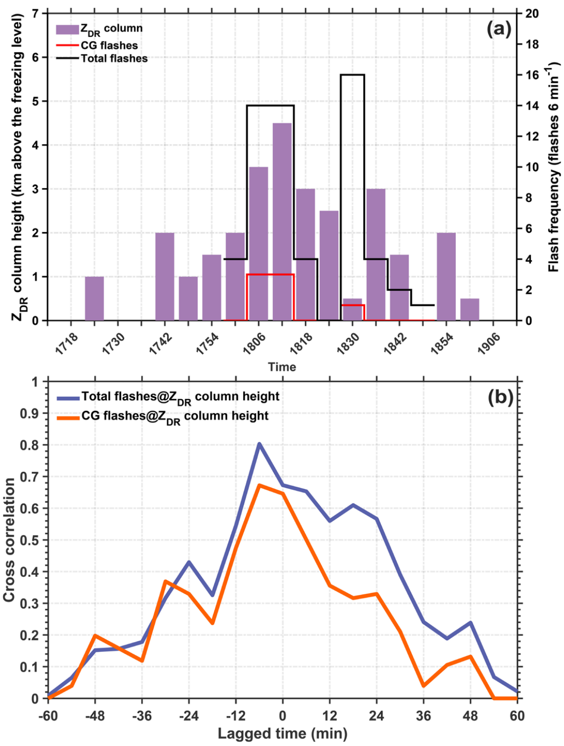

https://doi.org/10.5194/egusphere-2024-4069
Preprint. Discussion started: 16 January 2025

Figure 8. (a) The variation in the Z_{DR} column height with time. The purple bars indicate the heights of the Z_{DR} columns. The black (red) stepped line indicates the total flashes (CG flashes) from LFEDA, and the lightning flash frequency is counted every 6 minutes. (b) Cross-correlation between flash frequency and Z_{DR} column height; the blue and orange lines indicate the total flashes and CG flashes, respectively.

Figure 9 shows the relationship between lightning activity and the Z_{DR} column volume, and the variation trend in the second peak of lightning activity is indistinguishable via the variation trend in the Z_{DR} column volume (Figure 9a); this finding is similar to that shown in Figure 8a. The highest correlation coefficient between the lightning activity and Z_{DR} column volume is improved (~0.84 for the total flashes and 0.75 for CG flashes); specifically, the variation trend of the Z_{DR} column height can be used to predict the lightning activity (total flashes) after 6 minutes (Figure 9b).

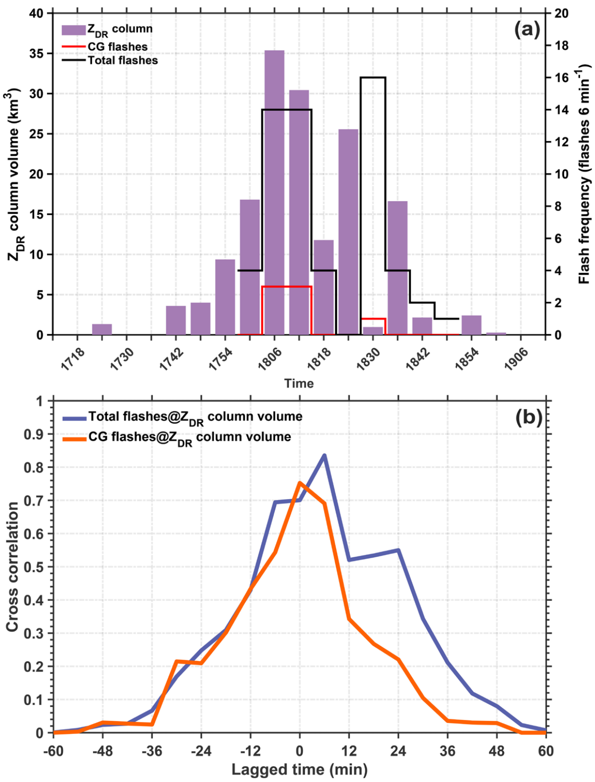

Figure 9. The same as in Figure 8 but for the Z_{DR} column volume.

3.4. Relationship between lightning activity and ice (liquid) microphysics

https://doi.org/10.5194/egusphere-2024-4069
Preprint. Discussion started: 16 January 2025

The microphysical characteristics of ice or liquid should exhibit a strong relationship with lightning activity on the basis of a noninductive charging mechanism. As expected, Figure 10 indicates that the variation in the rain-water content above the freezing level within the cloud can be better used to forecast lightning activity (total flashes) than can the variation in the Z_{DR} column volume. The highest correlation coefficient between the lightning activity (total flashes) and supercooled liquid water reaches approximately 0.93, and the lightning activity lag time is 6 minutes.

Figure 11 shows that the variation in the ice or graupel content above the freezing level within the cloud can indicate the lightning activity (total flashes) in real time, and the highest correlation coefficient between the lightning activity (total flashes) and the ice content is 0.84~0.89. However, the graupel content above the freezing level within the cloud is the best indicator for forecasting lightning activity (CG flashes); the highest correlation coefficient between lightning activity (CG flashes) and the graupel content is approximately 0.86, and the trend of CG flashes lags behind the variation in graupel content above the freezing level within the cloud, with a lag time of 6 minutes.

Therefore, the content of supercooled liquid water within the cloud is the best proxy for forecasting lightning activity (total flashes) after 6 minutes; the graupel content above the freezing level within the cloud is the best proxy for forecasting the lightning activity (CG flashes) after 6 minutes.

https://doi.org/10.5194/egusphere-2024-4069
Preprint. Discussion started: 16 January 2025

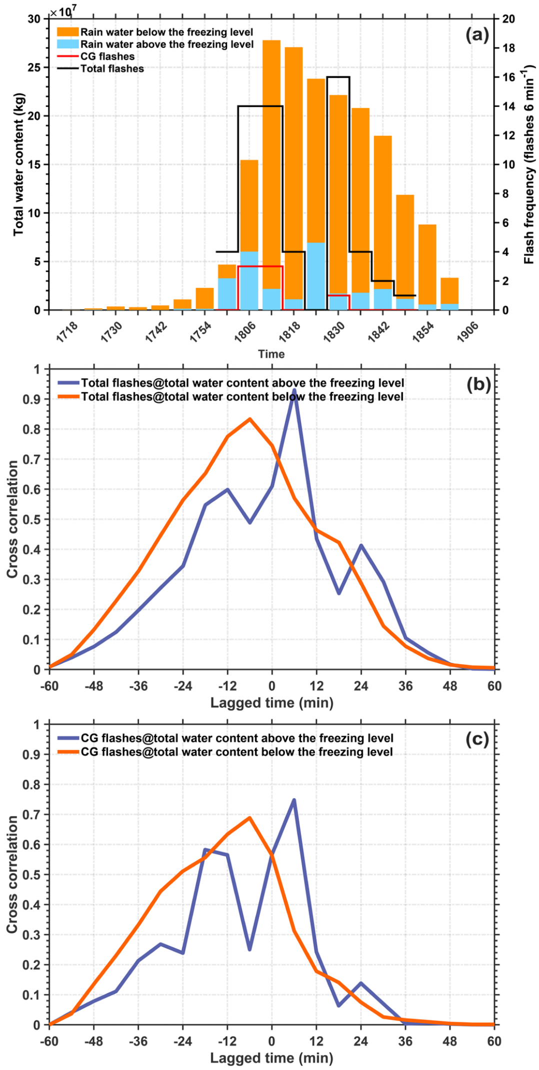

Figure 10. (a) The variation in total water content over time. The orange bars indicate rainwater below the freezing level. The blue bars indicate rainwater above the freezing level. (b) Cross-correlation between flash frequency and liquid microphysical characteristics; the blue and orange lines indicate the total flashes and CG flashes, respectively.

https://doi.org/10.5194/egusphere-2024-4069
Preprint. Discussion started: 16 January 2025

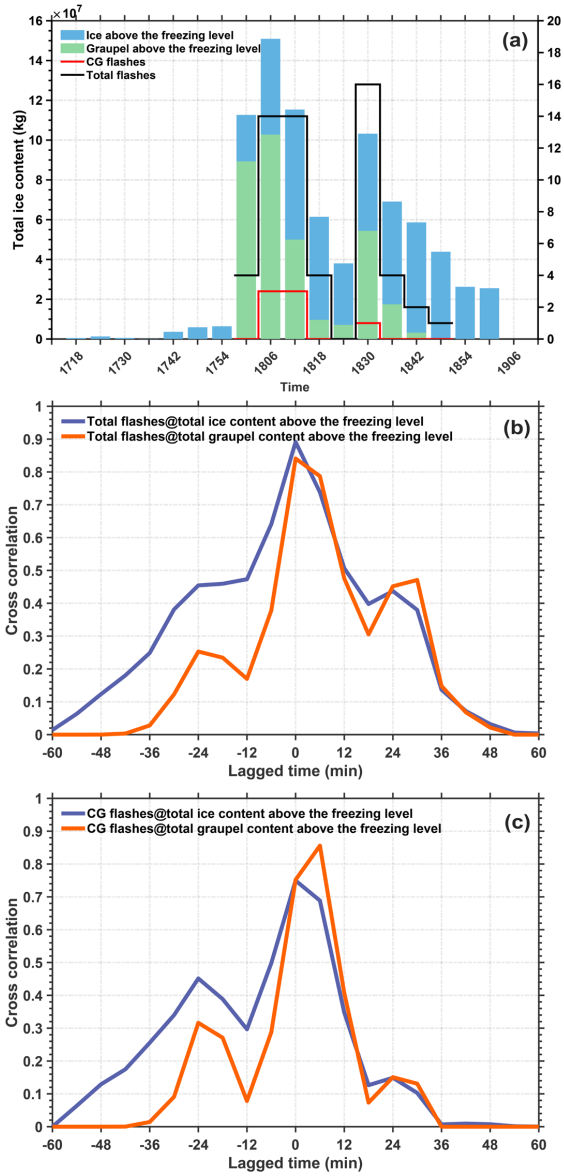

Figure 11. The same as in Figure 10 but for the total ice content.

4. Conclusion and discussion

The relationship between the polarimetric structure and lightning activity is investigated within an isolated thunderstorm cell during the cloud life cycle in this study. We focus on the proxies of cloud updrafts and supercooled liquid raindrops (Z_{DR} or K_{DP} columns) and the content of ice or rainwater, which have been demonstrated to be related to the variations in the number of lightning

https://doi.org/10.5194/egusphere-2024-4069
Preprint. Discussion started: 16 January 2025

flashes in previous studies (e.g., Carey and Rutledge, 2000; Hayashi et al., 2021; Sharma et al., 2024; Sharma, et al., 2021; van Lier-Walqui, et al., 2016). Therefore, the objective of this study is to clarify the sequence and interactions of these parameters for predicting lightning activity during the cloud life cycle and understanding the corresponding cloud microphysics.

To precisely identify and quantify the Z_{DR} or K_{DP} columns within an isolated thunderstorm during the whole cloud life cycle, the "3D mapping columns" method is established; it based on the morphology and high values of the Z_{DR} or K_{DP} columns in Cartesian grid data. The "3D mapping columns" method has advantages in identifying Z_{DR} columns in the initiation phase of convective clouds, avoiding the inappropriate threshold value of Z_H. The moment of occurrence of the first Z_{DR} column can be determined at least 36 minutes prior to the first lightning flash (Figure 5), which is a substantial lead time for forecasting the first lightning flash; notably, the numerical value was usually 4~6 minutes in previous studies (e.g., Gremillion and Orville, 1999; Vincent et al., 2003; Mosier, et al., 2011).

The volume and height of Z_{DR} columns are quantified via the "3D mapping columns" method, and the correlation coefficient indicates that the volume of the Z_{DR} column is better for forecasting lightning activity than is the column height. In addition, both the volume and height of a Z_{DR} column have some limitations in forecasting lightning activity, except during the early phase. This phenomenon is similar to the results of Sharma et al. (2024). In their study, the correlation coefficient between the Z_{DR} column volume and total flash rate generally monotonically decreased after initial lightning jump, and the volume of the K_{DP} columns exhibited relatively high co-variability with the total flash rate, except in the early phase. The time lag between reported between the formation of the Z_{DR} column and that of the K_{DP} column was consistent with the results of this study, indicating the different formation mechanisms of the Z_{DR} and K_{DP} columns described in Section 1.

As shown in Figure 4 and discussed in Section 3.1, we hypothesize that the K_{DP} column may form on the basis of the raindrops (1–2 mm) that shed from hailstones melting in the warm-phase region of clouds, which then recirculate into the updrafts and are lifted to the mixed-phase region. This is different from the hypothesis proposed in previous studies (e.g., (Bringi, et al., 1996, Hubbert, et al., 1998, Loney, et al., 2002)). Thus, the presence of many or large hailstones in supercells may

https://doi.org/10.5194/egusphere-2024-4069
Preprint. Discussion started: 16 January 2025

result in robust K_{DP} columns (e.g., (Sharma, et al., 2024)); in contrast, short lifetimes and weak dynamics within isolated thunderstorm cells in this study result in single-moment K_{DP} column.

Notably, our results indicate that the content of supercooled liquid water is the best variable for forecasting lightning activity (total flashes); the correlation coefficient is approximately 0.94, and the lead time is 6 minutes. For CG flash forecasting, the content of graupel displays the highest correlation coefficient (~0.86) with lightning activity, and the lead time is also 6 minutes. Similar results were reported by Carey and Rutledge (2000), suggesting that graupel particles are likely related to CG flash occurrence.

In our opinion, the prediction of lightning activity should involve the content of supercooled liquid water and graupel. Specifically, the first occurrence of the Z_{DR} column can be used to forecast lightning initiation as early as possible. Owing to the time lag between the formation of the Z_{DR} and K_{DP} columns, the signatures of the Z_{DR} and K_{DP} columns should be coupled to retrieve dynamic information instead of lightning activity; specifically, the Z_{DR} column is only suitable for the early phase of cloud development. We bridged the polarimetric structure (four important parameters provided in previous studies) and lightning activity on the basis of observations of a thermodynamically dominated isolated thunderstorm cell (the variation curve is conceptualized in Figure 12).

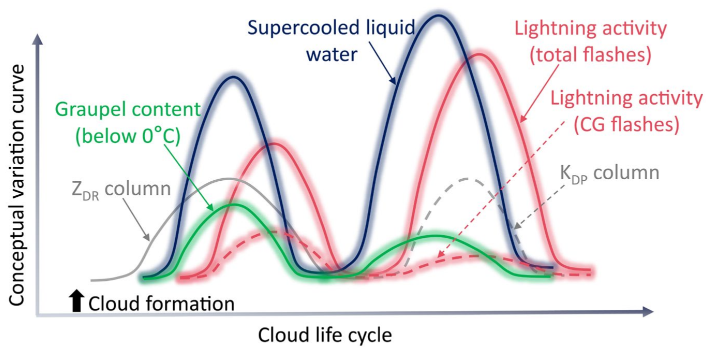

Figure 12. A conceptual model bridging the polarimetric structure and lightning activity.

Notably, the variation in the Z_H intensity and liquid water content within the Z_{DR} columns can be used to predict lightning activity during the cloud life cycle, and the former is a better preditor. However, this result is novel and has not been reported previously; therefore, substantial investigations should be performed to verify this finding in the future. Although this study is based

https://doi.org/10.5194/egusphere-2024-4069
Preprint. Discussion started: 16 January 2025

on the results of previous studies (e.g., Carey and Rutledge, 2000; Krause and Klaus, 2024; Sharma et al., 2024; Sharma, et al., 2021; Snyder, et al., 2015; van Lier-Walqui, et al., 2016; Woodard et al., 2012), more types of thunderstorms and more samples should be analysed to reduce the probability of uncertainty in our study.

Acknowledgments

The authors acknowledge the Guangzhou Institute of Tropical and Marine Meteorology for collecting and archiving the radar observations. And authors also acknowledge the State Key Laboratory of Severe Weather, Chinese Academy of Meteorological Sciences & Laboratory of Lightning Physics and Protection Engineering for three-dimensional lightning location data.

Financial support

This research has been supported by the National Natural Science Foundation of China (grant nos. 42175090 and 42305079), the China Postdoctoral Science Foundation (grant no. 2023M730619), the Natural Science Foundation of Sichuan Province (grant no. 2024NSFSC0771), and the Scientific Research Fund of Chengdu University of Information Technology (grant nos. KYTZ202213, KYQN202301, and KYQN202307).

Author contributions:

Conceptualization: CZ and YZ. Data curation: CZ, YZ, DZ, SD, and WY. Formal analysis: CZ, YZ, XP, and YD. Funding acquisition: YZ and CZ. Investigation: CZ, YZ, and XP. Methodology: CZ, YZ, HZ, ZL, and DZ. Project administration: YZ. Resources: CZ and YZ. Software: CZ, HZ, and ZL. Supervision: YZ. Validation: CZ and YZ. Visualization: CZ and YZ. Writing (original draft): CZ, YZ, and XP.

Competing interests:

The contact author has declared that none of the authors has any competing interests.

Data and materials availability: All data in this study can be obtained from an open repository Figshare (Zhao, 2024).

https://doi.org/10.5194/egusphere-2024-4069
Preprint. Discussion started: 16 January 2025

References

Amiot, C. G., Carey, L. D., Roeder, W. P., McNamara, T. M. and Blakeslee, R. J.: C-band Dual-Polarization Radar Signatures of Wet Downbursts around Cape Canaveral, Florida. Weather and Forecasting, 34(1): 103-131, 10.1175/waf-d-18-0081.1, 2019.

Baker, M. B., Blyth, A. M., Christian, H. J., Latham, J., Miller, K. L. and Gadian, A. M.: Relationships between lightning activity and various thundercloud parameters: satellite and modelling studies. Atmospheric Research, 51: 221-236, 10.1016/S0169-8095(99)00009-5, 1999.

Baker, M. B., Christian, H. J. and Latham, J.: A computational study of the relationships linking lightning frequency and other thundercloud parameters. Quarterly Journal of the Royal Meteorological Society, 121(527): 1525-1548, 10.1002/qj.49712152703, 1995.

Braham, R. R. Jr.: The cloud physics of weather modification. Part 1: Scientific basis. WMO Bulletin, 35, 215–221, 1986.

Bringi, V. N. and Chandrasekar, V.: Polarimetric Doppler Weather Radar: Principles and Applications. Cambridge University Press, Cambridge. 2001.

Bringi, V. N., Knupp, K., Detwiler, A., Liu, L., Caylor, I. J. and Black, R. A.: Evolution of a Florida Thunderstorm during the Convection and Precipitation/Electrification Experiment: The Case of 9 August 1991. Monthly Weather Review, 125(9): 2131-2160, https://doi.org/10.1175/1520-0493(1997)125<2131:EOAFTD>2.0.CO;2, 1997.

Bringi, V. N., Liu, L., Kennedy, P. C., Chandrasekar, V. and Rutledge, S. A.: Dual Multiparameter Radar Observations of Intense Convective Storms: The 24 June 1992 Case Study. Meteorology and Atmospheric Physics, 59: 3-31, 10.1007/BF01031999, 1996.

Bruning, E. C. and MacGorman, D. R.: Theory and Observations of Controls on Lightning Flash Size Spectra. Journal of the Atmospheric Sciences, 70(12): 4012-4029, 10.1175/jas-d-12-0289.1, 2013.

Carey, L. D. and Rutledge, S. A.: A Multiparameter Radar Case Study of the Microphysical and Kinematic Evolution of a Lightning Producing Storm. Meteorology and Atmospheric Physics, 59(1): 33-64, 10.1007/BF01032000, 1996.

Carey, L. D. and Rutledge, S. A.: The Relationship between Precipitation and Lightning in Tropical Island Convection: A C-Band Polarimetric Radar Study. Monthly Weather Review, 128(8): 2687-2710, 10.1175/1520-0493(2000)128<2687:TRBPAL>2.0.CO;2, 2000.

Deierling, W. and Petersen, W. A.: Total lightning activity as an indicator of updraft characteristics. Journal of Geophysical Research: Atmospheres, 113(D16), 10.1029/2007jd009598, 2008.

Deierling, W., Petersen, W. A., Latham, J., Ellis, S. and Christian, H. J.: The relationship between lightning activity and ice fluxes in thunderstorms. Journal of Geophysical Research: Atmospheres, 113(D15), 10.1029/2007jd009700, 2008.

Fan, X. P., Zhang, Y. J., Zheng, D., Zhang, Y., Lyu, W. T., Liu, H. Y. and Xu, L. T.: A New Method of Three-Dimensional Location for Low-Frequency Electric Field Detection Array. Journal of Geophysical Research: Atmospheres, 123(16): 8792-8812, 10.1029/2017jd028249, 2018.

Fridlind, A. M., van Lier-Walqui, M., Collis, S., Giangrande, S. E., Jackson, R. C., Li, X., Matsui, T., Orville, R., Picel, M. H., Rosenfeld, D., Ryzhkov, A., Weitz, R. and Zhang, P.: Use of polarimetric radar measurements to constrain simulated convective cell evolution: a pilot study with Lagrangian tracking. Atmospheric Measurement Techniques, 12(6): 2979-3000, 10.5194/amt-12-2979-2019, 2019.

https://doi.org/10.5194/egusphere-2024-4069
Preprint. Discussion started: 16 January 2025

Gatlin, P. N. and Goodman, S. J.: A Total Lightning Trending Algorithm to Identify Severe Thunderstorms. Journal of Atmospheric and Oceanic Technology, 27(1): 3-22, 10.1175/2009jtecha1286.1, 2010.

Gremillion, M. S., and Orville, R. E.: Thunderstorm Characteristics of Cloud-to-Ground Lightning at the Kennedy Space Center, Florida: A Study of Lightning Initiation Signatures as Indicated by the WSR-88D. Weather and Forecasting, 14: 640-649, 1999.

Goodman, S. J., Blakeslee, R., Christian, H., Koshak, W., Bailey, J., Hall, J., McCaul, E., Buechler, D., Darden, C., Burks, J., Bradshaw, T. and Gatlin, P.: The North Alabama Lightning Mapping Array: Recent severe storm observations and future prospects. Atmospheric Research, 76(1-4): 423-437, 10.1016/j.atmosres.2004.11.035, 2005.

Hayashi, S., Umehara, A., Nagumo, N. and Ushio, T.: The relationship between lightning flash rate and ice-related volume derived from dual-polarization radar. Atmospheric Research, 248, 10.1016/j.atmosres.2020.105166, 2021.

Helmus, J. J. and Collis, S. M.: The Python ARM Radar Toolkit (Py-ART), a Library for Working with Weather Radar Data in the Python Programming Language. Journal of Open Research Software, 4(1), 10.5334/jors.119, 2016.

Herzegh, P. H. and Jameson, A. R.: Observing Precipitation through Dual-Polarization Radar Measurements. Bulletin American Meteorological Society, 73(9): 1365-1376, 10.1175/1520-0477(1992)073<1365:OPTDPR>2.0.CO;2, 1992.

Homeyer, C. R. and Kumjian, M. R.: Microphysical Characteristics of Overshooting Convection from Polarimetric Radar Observations. Journal of the Atmospheric Sciences, 72(2): 870-891, 10.1175/jas-d-13-0388.1, 2015.

Hu, J. and Ryzhkov, A.: Climatology of the Vertical Profiles of Polarimetric Radar Variables and Retrieved Microphysical Parameters in Continental/Tropical MCSs and Landfalling Hurricanes. Journal of Geophysical Research: Atmospheres, 127(5), 10.1029/2021jd035498, 2022.

Hubbert, J., Bringi, V. N., Carey, L. D. and Bolen, S.: CSU-CHILL Polarimetric Radar Measurements from a Severe Hail Storm in Eastern Colorado. Journal of Applied Meteorology and Climatology, 37(8): 749-775, 10.1175/1520-0450(1998)037<0749:CCPRMF>2.0.CO;2, 1998.

Hubbert, J. C., Wilson, J. W., Weckwerth, T. M., Ellis, S. M., Dixon, M. and Loew, E.: S-Pol's Polarimetric Data Reveal Detailed Storm Features (and Insect Behavior). Bulletin of the American Meteorological Society, 99(10): 2045-2060, 10.1175/bams-d-17-0317.1, 2018.

Krause, J. and Klaus, V.: Identifying ZDR Columns in Radar Data with the Hotspot Technique. Weather and Forecasting, 39(3): 581-595, 10.1175/waf-d-23-0146.1, 2024.

Kumjian, M.: Principles and applications of dual-polarization weather radar. Part I: Description of the polarimetric radar variables. Journal of Operational Meteorology, 1(19): 226-242, 10.15191/nwajom.2013.0119, 2013a.

Kumjian, M.: Principles and applications of dual-polarization weather radar. Part II: Warm- and cold-season applications. Journal of Operational Meteorology, 1(20): 243-264, 10.15191/nwajom.2013.0120, 2013b.

Kumjian, M.: Principles and applications of dual-polarization weather radar. Part III: Artifacts. Journal of Operational Meteorology, 1(21): 265-274, 10.15191/nwajom.2013.0121, 2013c.

Kumjian, M. R., Khain, A. P., Benmoshe, N., Ilotoviz, E., Ryzhkov, A. V. and Phillips, V. T. J.: The

https://doi.org/10.5194/egusphere-2024-4069
Preprint. Discussion started: 16 January 2025

Anatomy and Physics of ZDR Columns: Investigating a Polarimetric Radar Signature with a Spectral Bin Microphysical Model. Journal of Applied Meteorology and Climatology, 53(7): 1820-1843, 10.1175/jamc-d-13-0354.1, 2014.

Lang, T. J. and Rutledge, S. A.: A Framework for the Statistical Analysis of Large Radar and Lightning Datasets: Results from STEPS 2000. Monthly Weather Review, 139(8): 2536-2551, 10.1175/mwr-d-10-05000.1, 2011.

Latham, J. and Dye, J. E.: Calculations on the electrical development of a small thunderstorm. Journal of Geophysical Research: Atmospheres, 94(D11): 13141-13144, https://doi.org/10.1029/JD094iD11p13141, 1989.

Li, H., Moisseev, D., Luo, Y., Liu, L., Ruan, Z., Cui, L. and Bao, X.: Assessing specific differential phase (KDP)-based quantitative precipitation estimation for the record- breaking rainfall over Zhengzhou city on 20 July 2021. Hydrology and Earth System Sciences, 27(5): 1033-1046, 10.5194/hess-27-1033-2023, 2023.

Li, H., Yin, J. and Kumjian, M.: Z Backwards Arc: Evidence of Multi-Directional Size Sorting in the Storm Producing 201.9 mm Hourly Rainfall. Geophysical Research Letters, 51(10): e2024GL109192, https://doi.org/10.1029/2024GL109192, 2024.

Liu, D., Li, F., Qie, X., Sun, Z., Wang, Y., Yuan, S., Sun, C., Zhu, K., Wei, L., Lyu, H. and Jiang, R.: Charge Structure and Lightning Discharge in a Thunderstorm Over the Central Tibetan Plateau. Geophysical Research Letters, 51(16): e2024GL109602, https://doi.org/10.1029/2024GL109602, 2024.

Liu, Z., Zheng, D., Guo, F., Zhang, Y., Zhang, Y., Wu, C., Chen, H. and Han, S.: Lightning activity and its associations with cloud structures in a rainstorm dominated by warm precipitation. Atmospheric Research, 246, 10.1016/j.atmosres.2020.105120, 2020.

Loney, M. L., Zrnić, D. S., Straka, J. M. and Ryzhkov, A. V.: Enhanced Polarimetric Radar Signatures above the Melting Level in a Supercell Storm. Journal of Applied Meteorology, 41(12): 1179-1194, https://doi.org/10.1175/1520-0450(2002)041<1179:EPRSAT>2.0.CO;2, 2002.

López, R. E. and Aubagnac, J.-P.: The lightning activity of a hailstorm as a function of changes in its microphysical characteristics inferred from polarimetric radar observations. Journal of Geophysical Research: Atmospheres, 102(D14): 16799-16813, https://doi.org/10.1029/97JD00645, 1997.

Marshall, T. C., Rust, W. D. and Stolzenburg, M.: Electrical structure and updraft speeds in thunderstorms over the southern Great Plains. Journal of Geophysical Research: Atmospheres, 100(D1): 1001-1015, https://doi.org/10.1029/94JD02607, 1995.

Mitzeva, R. and Saunders, C. P. R.: Thunderstorm charging: calculations of the effect of ice crystal size and graupel velocity. Journal of Atmospheric and Terrestrial Physics, 52(4): 241-245, https://doi.org/10.1016/0021-9169(90)90090-A, 1990.

Mosier, R. M., Schumacher, C., Orville, R. E. and Carey, L. D.: Radar Nowcasting of Cloud-to-Ground Lightning over Houston, Texas. Weather and Forecasting, 26(2): 199-212, https://doi.org/10.1175/2010WAF2222431.1, 2011.

Pruppacher, H. R., and Klett, J. D.: Microphysics of Clouds and Precipitation. 2d ed. Kluwer Academic, 954 pp., 1997.

Qie, X., Yu, Y., Liu, X., Guo, C., Wang, D., Watanabe, T. and Ushio, T.: Charge analysis on lightning discharges to the ground in Chinese inland plateau (close to Tibet). Ann. Geophys., 18(10):

https://doi.org/10.5194/egusphere-2024-4069
Preprint. Discussion started: 16 January 2025

1340-1348, 10.1007/s00585-000-1340-z, 2000.

Reynolds, S. E., Brook, M. and Gourley, M. F.: THUNDERSTORM CHARGE SEPARATION. Journal of Atmospheric Sciences, 14(5): 426-436, https://doi.org/10.1175/1520-0469(1957)014<0426:TCS>2.0.CO;2, 1957.

Rison, W., Thomas, R. J., Krehbiel, P. R., Hamlin, T. and Harlin, J.: A GPS-based three-dimensional lightning mapping system: Initial observations in central New Mexico. Geophysical Research Letters, 26(23): 3573-3576, https://doi.org/10.1029/1999GL010856, 1999.

Rosenfeld, D., Lohmann, U., Raga, G. B., O'Dowd, C. D., Kulmala, M., Fuzzi, S., Reissell, A. and Andreae, M. O.: Flood or Drought: How Do Aerosols Affect Precipitation? Science, 321(5894): 1309-1313, doi:10.1126/science.1160606, 2008.

Saunders, C.: Charge Separation Mechanisms in Clouds. Space Science Reviews, 137(1): 335-353, 10.1007/s11214-008-9345-0, 2008.

Seliga, T. A. and Bringi, V. N.: Potential Use of Radar Differential Reflectivity Measurements at Orthogonal Polarizations for Measuring Precipitation. Journal of Applied Meteorology and Climatology, 15(1): 69-76, https://doi.org/10.1175/1520-0450(1976)015<0069:PUORDR>2.0.CO;2, 1976.

Sharma, M., Tanamachi, R. L. and Bruning, E. C.: Investigating Temporal Characteristics of Polarimetric and Electrical Signatures in Three Severe Storms: Insights from the VORTEX-Southeast Field Campaign. Monthly Weather Review, 152(7): 1511-1536, https://doi.org/10.1175/MWR-D-23-0144.1, 2024.

Sharma, M., Tanamachi, R. L., Bruning, E. C. and Calhoun, K. M.: Polarimetric and Electrical Structure of the 19 May 2013 Edmond–Carney, Oklahoma, Tornadic Supercell. Monthly Weather Review, 149(7): 2049-2078, https://doi.org/10.1175/MWR-D-20-0280.1, 2021.

Shi, D., Zheng, D., Zhang, Y., Zhang, Y., Huang, Z., Lu, W., Chen, S. and Yan, X.: Low-frequency E-field Detection Array (LFEDA)—Construction and preliminary results. Science China Earth Sciences, 60(10): 1896-1908, 10.1007/s11430-016-9093-9, 2017.

Snyder, J. C., Bluestein, H. B., Dawson II, D. T. and Jung, Y.: Simulations of Polarimetric, X-Band Radar Signatures in Supercells. Part I: Description of Experiment and Simulated ρhv Rings. Journal of Applied Meteorology and Climatology, 56(7): 1977-1999, https://doi.org/10.1175/JAMC-D-16-0138.1, 2017.

Snyder, J. C., Ryzhkov, A. V., Kumjian, M. R., Khain, A. P. and Picca, J.: A ZDR Column Detection Algorithm to Examine Convective Storm Updrafts. Weather and Forecasting, 30(6): 1819-1844, https://doi.org/10.1175/WAF-D-15-0068.1, 2015.

Souza, J. C. S. and Bruning, E. C.: Assessment of Turbulence Intensity in Different Spots of Lightning Flash Propagation. Geophysical Research Letters, 48(21): e2021GL095923, https://doi.org/10.1029/2021GL095923, 2021.

Takahashi, T.: Riming Electrification as a Charge Generation Mechanism in Thunderstorms. Journal of Atmospheric Sciences, 35(8): 1536-1548, https://doi.org/10.1175/1520-0469(1978)035<1536:REAACG>2.0.CO;2, 1978.

Tuttle, J. D., Bringi, V. N., Orville, H. D. and Kopp, F. J.: Multiparameter Radar Study of a Microburst: Comparison with Model Results. Journal of Atmospheric Sciences, 46(5): 601-620, https://doi.org/10.1175/1520-0469(1989)046<0601:MRSOAM>2.0.CO;2, 1989.

van Lier-Walqui, M., Fridlind, A. M., Ackerman, A. S., Collis, S., Helmus, J., MacGorman, D. R., North, K., Kollias, P. and Posselt, D. J.: On Polarimetric Radar Signatures of Deep Convection for Model Evaluation: Columns of Specific Differential Phase Observed during MC3E. Monthly Weather Review, 144(2): 737-758, https://doi.org/10.1175/MWR-D-15-0100.1, 2016.

Vincent, B. R., Carey, L. D. Schneider, D., Keeter, K., and Gonski, R.: Using WSR-88D reflectivity data for the prediction of cloud-to-ground lightning: A central North Carolina study. Nat. Wea. Dig., 27: 35-44, 2003.

Williams, E., Boldi, B., Matlin, A., Weber, M., Hodanish, S., Sharp, D., Goodman, S., Raghavan, R. and Buechler, D.: The behavior of total lightning activity in severe Florida thunderstorms. Atmospheric Research, 51(3): 245-265, https://doi.org/10.1016/S0169-8095(99)00011-3, 1999.

Williams, E. R., Weber, M. E. and Orville, R. E.: The relationship between lightning type and convective state of thunderclouds. Journal of Geophysical Research: Atmospheres, 94(D11): 13213-13220, https://doi.org/10.1029/JD094iD11p13213, 1989.

Woodard, C. J., Carey, L. D., Petersen, W. A., and Roeder, W. P.: Operational utility of dual-polarization variables in lightning initiation forecasting, Electronic J. Operational Meteor., 13, 79-102, 2012.

Yan, M., Guo, C., Ge, Z.: Numerical study of cloud dynamic-electrification in an axisymmetric, time-dependent cloud model. I: Theory and model. ACTA GEOPHYSICA SINICA, 39: 52-64, 1996a.

Yan, M., Guo, C., Ge, Z.: Numerical study of cloud dynamic-electrification in an axisymmetric, time-dependent cloud model. II: Calculation results. ACTA GEOPHYSICA SINICA, 39: 65-77, 1996b.

Zhang, Y., Sun, A., Yan, M., Guo, F., Qie, X., Huang, M.: Numerical modeling for effects of electric activity during thunderstorms upon the growth of hail particles. Chinese Journal of Geophysics, 47(1): 25-32, 2004a.

Zhang, Y., Dong, W., Zhao, Y., Zhang, G., Zhang, H., Chen, C. and Zhang, T.: Study of charge structure and radiation characteristic of intracloud discharge in thunderstorms of Qinghai-Tibet Plateau. Science in China Series D: Earth Sciences, 47(1): 108-114, 10.1007/BF02880986, 2004b.

Zhang, Y., Yan, M., Sun, A., Guo, F.: Thunderstorm Electricity, China Meteorology Press, Beijing, 384 pp., 2009.

Zhao, C.: Data for "Bridging the polarimetric structure and lightning activity of an isolated thunderstorm during the cloud life cycle". Figshare. [Dataset]. https://doi.org/10.6084/m9.figshare.28070105.v1, 2024.

Zhao, C., Zhang, Y., Zheng, D., Li, H., Du, S., Peng, X., Liu, X., Zhao, P., Zheng, J. and Shi, J.: Technical note: On the ice microphysics of isolated thunderstorms and non-thunderstorms in southern China – a radar polarimetric perspective. Atmospheric Chemistry and Physics, 24(20): 11637-11651, 10.5194/acp-24-11637-2024, 2024.

Zhao, C., Zhang, Y., Zheng, D., Liu, X., Zhang, Y., Fan, X., Yao, W. and Zhang, W.: Using Polarimetric Radar Observations to Characterize First Echoes of Thunderstorms and Nonthunderstorms: A Comparative Study. Journal of Geophysical Research: Atmospheres, 127(23): e2022JD036671, https://doi.org/10.1029/2022JD036671, 2022.

Zhao, C., Zhang, Y., Zheng, D., Zhou, Y., Xiao, H. and Zhang, X.: An improved hydrometeor identification method for X-band dual-polarization radar and its application for one summer Hailstorm over Northern China. Atmospheric Research, 245: 105075,

https://doi.org/10.1016/j.atmosres.2020.105075, 2020.
Zhao, C., Zheng, D., Zhang, Y., Liu, X., Zhang, Y., Yao, W. and Zhang, W.: Turbulence Characteristics of Thunderstorms Before the First Flash in Comparison to Non-Thunderstorms. Geophysical Research Letters, 48(18): e2021GL094821, https://doi.org/10.1029/2021GL094821, 2021.
Zheng, D. and Zhang, Y.: New Insights Into the Correlation Between Lightning Flash Rate and Size in Thunderstorms. Geophysical Research Letters, 48(24): e2021GL096085, https://doi.org/10.1029/2021GL096085, 2021.
Zrnić, D. S.: Three-body scattering produces precipitation signature of special diagnostic value. Radio Science, 22(1): 76-86, https://doi.org/10.1029/RS022i001p00076, 1987.